Pesq. Vet. Bras. 46:e07830, 2026
DOI: 10.1590/1678-5150-PVB-7830

Case Report
Wildlife Medicine

Septic osteoarthritis caused by *Bacillus pumilus* in a green iguana (*Iguana iguana*)[1]

André A. Justo[2], Anna C.M. Ercolin[2], Pedro G.M. Rihs[2], Fredderico Garcia[2], Ricardo F. Strefezzi[2], Marcus A.R. Feliciano[2], Adriano B. Carregaro[2]*

Registros ORCID:
André Augusto Justo – https://orcid.org/0000-0002-9853-8575
Anna Carolina Mazeto Ercolin – https://orcid.org/0000-0002-5832-9015
Pedro Gustavo Macedo Rihs – https://orcid.org/0009-0005-8902-4862
Fredderico Garcia – https://orcid.org/0009-0006-8462-6327
Ricardo de Franscico Strefezzi – https://orcid.org/0000-0002-8810-2815
Marcus Antônio Rossi Feliciano – https://orcid.org/0000-0003-4373-6539
Adriano Bonfim Carregaro – https://orcid.org/0000-0002-0580-0467

ABSTRACT.- Justo AA, Ercolin ACM, Rihs PGM, Garcia F, Strefezzi RF, Feliciano MAR, Carregaro AB. **Septic osteoarthritis caused by *Bacillus pumilus* in a green iguana (*Iguana iguana*).** *Pesquisa Veterinária Brasileira 46:e07830, 2026.* Departamento de Medicina Veterinária, Faculdade de Zootecnia e Engenharia de Alimentos, Universidade de São Paulo, Av. Duque de Caxias Norte 225, Jardim Elite, Pirassununga, SP 13635-900, Brazil. E-mail: carregaro@usp.br

A green iguana (*Iguana iguana*) was presented with acute swelling of the left knee and reluctance to flex the joint. Diagnostic imaging findings were consistent with septic osteoarthritis. They included progressive osteolysis and osteoproliferative changes affecting the distal femoral and proximal tibial epiphyses, as well as intra-articular effusion, which were monitored using radiography and ultrasonography. Bacteriological culture of synovial fluid, followed by matrix-assisted laser desorption/ionization time-of-flight mass spectrometry (MALDI-TOF MS), identified *Bacillus pumilus*, a saprophytic bacterium rarely associated with disease. Despite antimicrobial therapy guided by susceptibility testing, the osteoarticular lesions progressed, ultimately requiring limb amputation. Histopathological examination confirmed chronic granulomatous osteomyelitis. The patient recovered uneventfully, with no recurrence of lesions during a 1-year follow-up. Serial imaging was essential for monitoring disease progression, refining differential diagnoses, and guiding surgical decision-making. To the best of the authors' knowledge, this is the first report of osteoarticular infection caused by *B. pumilus* in a reptile, highlighting the potential role of opportunistic environmental pathogens in the pathogenesis of musculoskeletal disease in lizards.

INDEX TERMS: Bacteria, infection, radiography, ultrasonography.

RESUMO.- [**Osteoartrite séptica causada por *Bacillus pumilus* em uma iguana-verde (*Iguana iguana*).**] Uma iguana-verde (*Iguana iguana*) apresentou edema agudo no joelho esquerdo e relutância em flexionar a articulação. Achados de imagens foram consistentes com osteoartrite séptica, incluindo alterações osteolíticas e osteoproliferativas progressivas na epífise femoral distal e tibial proximal, bem como efusão intra-articular, as quais foram acompanhadas radiografica e ultrassonograficamente. A cultura bacteriológica do líquido sinovial, seguida de espectrometria de massas por ionização/dessorção a laser assistida por matriz com analisador de tempo de voo (MALDI-TOF MS), identificou *Bacillus pumilus*, uma bactéria saprofítica raramente associada à doença. Apesar da terapia antimicrobiana guiada por testes de sensibilidade, observou-se progressão das lesões osteoarticulares, e procedeu-se à amputação do membro. O exame histopatológico confirmou osteomielite granulomatosa crônica. O paciente recuperou-se sem complicações no pós-operatório, sem recidiva das lesões após um ano de acompanhamento. Exames de imagem seriados foram fundamentais para avaliar a progressão

[1] Received on April 2, 2026.
Accepted for publication on July 1, 2026.
[2] Departamento de Medicina Veterinária, Faculdade de Zootecnia e Engenharia de Alimentos, Universidade de São Paulo (USP), Av. Duque de Caxias Norte 225, Jardim Elite, Pirassununga, SP 13635-900, Brazil. *Corresponding author: carregaro@usp.br

das lesões e refinar os diagnósticos diferenciais, auxiliando na decisão cirúrgica. Até o presente momento, não há relatos na literatura de infecção osteoarticular causada por *B. pumilus* em répteis, destacando o potencial papel de patógenos ambientais oportunistas na patogenia de doenças musculoesqueléticas em lagartos.

TERMOS DE INDEXAÇÃO: Bactéria, infecção, radiografia, ultrassom.

INTRODUCTION

Green iguanas (*Iguana iguana*) are among the most commonly maintained lizard species in captivity, owing to their adaptability to *ex situ* settings and the extensive literature on their husbandry. They are widely used in anesthesia and pain research (Ghussn et al. 2024, Bisetto et al. 2025, Justo et al. 2026), as well as in physiological and comparative studies (Filogonio et al. 2022, Guagnoni et al. 2024). They are also prominent in the pet trade (Robinson et al. 2015). A recent study found green iguanas to be the most prevalent of 14 lizard species presented to a veterinary referral center from 2000 to 2023 (Gise et al. 2025), further emphasizing their contribution to advances in reptile medicine.

Musculoskeletal disorders are relatively common in captive lizards and include fractures, metabolic bone disease, and osteomyelitis or septic arthritis (Knafo 2019). While considerable attention has been devoted to the etiology and clinical management of bone disease secondary to nutritional imbalances in captive animals, fewer reports are available on osteomyelitis in lizards. Among infectious agents, *Mycobacterium* spp. have been identified as a major concern in limb infections (Kramer 2006) and have been reported to cause osteomyelitis of the knee joint in a bearded dragon (*Pogona vitticeps*) (Vaillard et al. 2021). Similarly, *Klebsiella* spp. have been associated with osteolytic-osteoproliferative spinal lesions in the same species (Vetere et al. 2021). These reports indicate a poor prognosis for lizards affected by this condition, with outcomes including euthanasia (Vaillard et al. 2021) and death (Kramer 2006). Furthermore, they highlight the potential role of opportunistic pathogens in the development of osteomyelitis in reptiles.

Opportunistic pathogens are well-recognized causes of infection in human medicine, particularly in immunocompromised patients. For instance, *Bacillus pumilus*, a Gram-positive, spore-forming bacterium widely distributed in soil, air, water, and food, is commonly used in agriculture as a biological control agent (Celandroni et al. 2016). Although rarely pathogenic, it has been reported to cause severe disease in humans, including septic arthritis (Shivamurthy et al. 2016), cellulitis (Neves-Maia et al. 2024), and sepsis (Kimouli et al. 2012). In veterinary medicine, its role as an etiological agent is less well characterized, although it has been identified as an opportunistic pathogen in the bovine uterus associated with endometritis (Ballas et al. 2023). The aim of this study was to report the first case of septic osteoarthritis caused by *B. pumilus* in a green iguana, thereby expanding the evidence supporting the role of saprophytic bacteria as opportunistic agents in musculoskeletal infections in lizards.

CASE REPORT

Ethical approval. The animal described in this case report was housed at the Reptile Bioterium of the “Faculdade de Zootecnia e Engenharia de Alimentos” (School of Animal Science and Food Engineering – FZEA), “Universidade de São Paulo” (USP), which is registered with the “Conselho Nacional de Controle de Experimentação Animal” (Brazilian National Council for the Control of Animal Experimentation – CONCEA). Before the onset of the condition described herein, the animal was enrolled in a study approved by the Animal Care and Use Committee of FZEA-USP (CEUA no. 4923150823) and authorized by the “Sistema de Autorização e Informação em Biodiversidade” (Brazilian Biodiversity Information and Authorization System – SISBIO no. 79652-2). Following development of the limb infection, the animal was withdrawn from the study and subsequently received routine veterinary care independent of the experimental protocol.

An adult female green iguana (*Iguana iguana*) weighing 1 kg was referred to the veterinary hospital of FZEA-USP with a history of difficulty perching and left hindlimb swelling, both of which were first noted the previous day. The iguana was fed a diet consisting of dark leafy greens (80%; collard greens, arugula, and cress), vegetables (10%; chayote and carrots), fruits (5%; mango and pear), and hibiscus leaves (5%), supplemented with commercial reptile pellets (Megazoo, Brazil) and calcium carbonate (Homeopatia Ouro Preto, Brazil) on alternate days. Water was provided *ad libitum*. The animal was housed with another clinically healthy adult female green iguana in a 750-L enclosure (1.52 × 0.77 m). Ambient temperature was maintained between 27 and 30 °C and relative humidity between 50 and 60%. A 12-h light cycle was provided using a 26-W fluorescent lamp emitting UVA (30%) and UVB (5%) radiation (LuckyHerp, China). A basking spot maintained at 35–40 °C was provided by a 250-W incandescent bulb (Lumanti Lighting for Life, Brazil), which was operated twice daily from 8:00 to 10:00 and from 14:00 to 16:00.

The iguana showed no changes in appetite or attitude; however, physical examination revealed diffuse edema affecting the entire left hindlimb, particularly around the knee, with restricted flexion compared with the contralateral limb (Fig. 1). The animal also displayed defensive behavior during manipulation of the affected limb, consistent with pain. Additionally, superficial bilateral pedal lesions in an advanced stage of healing were observed, consistent with a history of hindlimb withdrawal latency testing within the previous six months. A complete blood count was performed (erythrocyte count, 0.92×10^6/µL; hemoglobin concentration, 9.5 g/dL; hematocrit, 27%; total plasma protein concentration, 6.6 g/dL; leukocyte count, 3,500/µL; heterophils, 2,765/µL; eosinophils, 70/µL; lymphocytes, 595/µL; monocytes, 70/µL), and the results were considered unremarkable for the species (Divers 1996). Meloxicam (Maxicam® 0.2%; Ourofino, Brazil) was administered at 0.2 mg/kg once daily (SID) SC, and radiographic and ultrasonographic examinations were scheduled for the following day. Based on the clinical findings, the differential diagnoses included trauma, neoplasia, and osteomyelitis. Radiographic examination was performed in the dorsoventral projection using a DIGIX WM digital system and an Altus 543 X-ray unit (SAWAE®) at 55 kV and 4 mAs, with a bone-processing algorithm. Mild soft tissue swelling adjacent to the left femorotibiopatellar joint was observed, but no fractures were identified (Fig. 2). Ultrasonographic examination was performed using a MyLab X8 Vet (Esaote®) device under physical restraint in the prone position with a multifrequency linear transducer set to 15.0 MHz. In B-mode, the femoral and tibial cortical surfaces appeared as fine, regular hyperechoic lines. Homogeneous echogenic material was observed within the left femorotibiopatellar joint space, suggestive of joint effusion (Fig. 5). Following aseptic preparation of the site, arthrocentesis of the affected joint was performed, and the aspirated material was submitted for bacterial culture, antimicrobial susceptibility testing, and microorganism identification by matrix-assisted laser desorption/ionization time-of-flight mass spectrometry (MALDI-ToF MS; Microflex® LT, Bruker). Mass spectra were acquired using FlexControl 3.4 software and analyzed with MBT Compass version 4.1.100. Cytological examination was not performed because of technical constraints. Pending further diagnostic results, the animal was maintained on meloxicam (0.2 mg/kg, SC, SID) for 10 days and enrofloxacin (Zelotril® 10%; Agener União, Brazil) administered at 10 mg/kg IM SID (Salvadori et al. 2016). Enrofloxacin treatment was continued until further clinical reassessment.

Follow-up imaging performed 20 days after the initial evaluation demonstrated progression of the osteoarticular disease and increased periarticular soft tissue volume. The distal epiphysis of the left femur showed cortical thinning, while the proximal epiphysis of the left tibia demonstrated radiolucent areas of bone lysis (Fig. 3). Ultrasonographically, irregular bone surfaces were observed, accompanied by adjacent echogenic areas consistent with bone proliferation and circumscribed cavitary defects suggestive of osteolysis. Heterogeneous echogenic material was present within the joint space and had increased in volume compared with the initial examination (Fig. 6). The presumptive diagnosis of septic osteoarthritis was subsequently confirmed by the isolation of *Bacillus pumilus* from the lesion. Antimicrobial susceptibility testing demonstrated susceptibility to amikacin, ampicillin, ceftriaxone, ciprofloxacin, chloramphenicol, and enrofloxacin. Given the progression of the osteoarticular lesions despite ongoing antimicrobial therapy, amikacin (250 mg/mL; Teuto, Brazil) was added at 5 mg/kg IM, followed by 2.5 mg/kg IM every 72 h (Stahl 2003), while enrofloxacin was maintained. A multimodal analgesic regimen consisting of meloxicam (0.2 mg/kg, SC, SID) and morphine (Dirmorf® 10 mg/mL; Cristália, Brazil) at 5 mg/kg IM SID for five days was also implemented. During treatment, the animal remained alert and active, maintained a normal appetite, and was in good body condition.

Ten days later (i.e., one month after the initial presentation), reduced mobility persisted, and joint edema had worsened despite ongoing treatment. A repeat radiographic examination revealed marked progression of the lesions, including further bone lysis of the distal femoral epiphysis and destruction of the proximal tibial epiphysis (Fig. 4). Similarly, ultrasonographic examination revealed loss of definition of the proximal tibial epiphysis and increased intra-articular volume containing heterogeneous material (Fig. 7). Given the poor prognosis and concerns regarding animal welfare, amputation of the left pelvic limb at the hip joint was elected. The procedure was performed under isoflurane anesthesia with neuraxial administration of bupivacaine (0.2 mL/kg; Neocaína®, Cristália, Brazil) according to a previously described technique (Ferreira & Mans 2019) and was completed without complications.

On gross inspection of the femorotibiopatellar region following amputation, both the distal femoral epiphysis and the proximal tibial epiphysis exhibited irregular surfaces with loss of normal bone definition, as well as marked accumulation of serosanguineous fluid. Material collected directly from the lesion during surgery was submitted for repeat bacteriological culture and identification by mass spectrometry, confirming infection by *B. pumilus*. Antimicrobial susceptibility testing revealed no changes from the previously reported susceptibility profile. Fragments of the distal femoral epiphysis and proximal tibial epiphysis were submitted for histopathological examination, and Gram staining was performed on histological sections in an attempt to identify intralesional bacteria. The bone tissue exhibited marked pathological alterations consistent with osteomyelitis. Microscopic examination revealed moderate periosteal lysis and proliferation, along with extensive fibroplasia replacing portions of the joint capsule, articular cartilage, and trabecular bone (Fig. 8-11). Multifocal granulomas were present within the fibrous tissue and consisted of central areas of necrotic debris and granulocytes surrounded by mononuclear and multinucleated giant cells (Fig. 12-13). The bone marrow was densely infiltrated or replaced by granulocytes (Fig. 14-16). Granulomas were also present in the subcutaneous tissue and muscle. Gram-positive structures morphologically consistent with bacteria were observed within the cytoplasm of multinucleated giant cells (Fig. 17). No histological evidence of neoplasia was identified.

Meloxicam, enrofloxacin, and amikacin were continued at the aforementioned dosages for an additional five days after surgery, resulting in a total of five weeks of enrofloxacin therapy and two weeks of amikacin therapy, with no postoperative complications. The animal remained in an isolated enclosure for postoperative care, during which it remained alert and active and maintained a normal appetite. The enclosure was modified by increasing the number of perches and lowering their height to support the species' natural climbing behavior. One year after amputation, there was no recurrence of infection elsewhere in the body, and the animal maintained satisfactory locomotor function.

DISCUSSION

Osteomyelitis in lizards primarily affects the appendicular skeleton and is radiographically characterized by radiolucent lytic regions, generally without significant new bone formation (Knafo 2019). In the present report, radiography revealed aggressive lysis extending distally into the femur and proximally into the tibia, in addition to localized soft tissue swelling. Proliferative bone changes were observed ultrasonographically and confirmed by histopathology. This mixed osteolytic-osteoproliferative pattern resembles previous reports of *Mycobacterium* spp.-associated osteomyelitis in the knee joint of a bearded dragon (Kramer 2006), supporting consideration of osteomyelitis among the differential diagnoses in lizards presenting with periosteal reactions. Ultrasonography also aided in identifying the infectious process as the primary clinical suspicion by demonstrating early joint effusion in the femorotibiopatellar joint. Although not routinely used in clinical practice, ultrasonography may provide additional diagnostic value in lizards with marked soft tissue enlargement, as joint effusion may not always be evident on radiographs (Holmes & Divers 2019).

Clinically, swelling of the knee was the most prominent finding, while the animal maintained normal appetite and behavior throughout the progression of the disease despite marked imaging abnormalities. This observation is consistent with previous reports in bearded dragons, in which clinical deterioration occurred only weeks after radiographic evidence of osteomyelitis (Kramer 2006, Vaillard et al. 2021). Therefore, the clinical status of affected lizards may not correlate with the severity of imaging findings, highlighting the importance of serial imaging in disease monitoring. In the present case, close monitoring of bone involvement may have contributed to the early recognition of disease progression, potentially preventing extension beyond the joint and systemic dissemination, as previously reported (Kramer 2006, Girling & Fraser 2007, Vaillard et al. 2021). However, the articular surface showed marked progression of osteolysis despite the early use of a broad-spectrum antibiotic followed by antimicrobial therapy based on *in vitro* susceptibility testing, including enrofloxacin and amikacin, both administered at recommended reptile dosages and reported to achieve therapeutic concentrations in bone tissue in other species (Ehinger et al. 2002, Thabit et al. 2019). One possible explanation is the granulomatous nature of the reptilian inflammatory response, which was also observed in the present case and may hinder antimicrobial penetration into affected bone (Knafo 2019). Early bone curettage and joint lavage with antimicrobials may warrant consideration in similar cases involving green iguanas to preserve limb function. Nonetheless, once advanced osteolysis has developed, restoration of joint function is unlikely, and surgical intervention, including arthrodesis or amputation, is recommended (Knafo 2019).

While the aggressive and progressive lytic alterations associated with soft tissue swelling were compatible with bone infection, definitive diagnosis requires microbiological culture and histopathological evaluation (Chinadurai & Devoe 2009), as performed in this case. In addition, as growth characteristics in culture have not enabled an infectious agent to be speciated in past lizard reports (Kramer 2006, Vetere al. 2021), mass spectrometry was carried out due to its high accuracy to taxonomically differentiate bacteria (Clark et al. 2013, Neves-Maia et al. 2024). Beyond mycobacterial infections (Kramer 2006, Girling & Fraser 2007, Vaillard et al. 2021), Gram-negative bacteria are most commonly associated with osteomyelitis in reptiles, including *Salmonella* spp. (Isaza et al. 2000, Knafo 2019) and *Klebsiella* spp. (Vetere et al. 2021). Although Gram-positive bacteria have also been implicated (Chinadurai & Devoe 2009), the identification of *B. pumilus*, a Gram-positive, ubiquitous, spore-forming bacterium, as the causative agent of granulomatous osteomyelitis in this green iguana highlights the potential role of soil-borne pathogens in osteomyelitis of captive lizards.

Contamination of the bacteriological culture was considered unlikely, as repeated cultures yielded consistent results, including samples obtained directly from the affected site during surgery. Repeated isolation of *B. pumilus* from the site of infection has been regarded as evidence supporting a pathogenic rather than contaminant role (Kimouli et al. 2012, Shivamurthy et al. 2016). With this in mind, *B. pumilus* is infrequently associated with disease; aside from its role in bovine endometritis (Ballas et al. 2023), most reports involve human patients, particularly those who are immunocompromised (Banerjee et al. 1988) or neonates (Kimouli et al. 2012), as well as individuals with a history of intravenous drug use (Neves-Maia et al. 2024) or major surgery (Borsa et al. 2016). In captive lizards, immunosuppression has been associated with poor husbandry practices and stress (Knafo 2019). While the housing conditions of the green iguanas maintained at the institution's Bioterium were in line with the recommendations for this species, stress cannot be entirely ruled out as a contributing factor to the observed infection, given that the animal had previously participated in an experimental protocol involving antinociceptive testing, which may have represented a potential stressor. The complete blood count was within normal limits and showed no evidence of a stress leukogram, typically characterized by leukocytosis with heterophilia and lymphopenia (Davis et al. 2008). However, the magnitude of stress-induced leukogram alterations has not been investigated in depth across reptile species (Heatley & Russell 2019), precluding definitive conclusions based solely on blood count results. That said, *B. pumilus* infections have also been reported, albeit rarely, in otherwise healthy people (Tena et al. 2007, Shivamurthy et al. 2016), suggesting that overt immunosuppression may not be a prerequisite for infection in the present iguana.

Regardless of whether host-related factors contributed to susceptibility, the presence of healing pedal lesions suggests a plausible route of infection, as the skin trauma may have served as a portal of entry for the bacteria and facilitated an ascending infection. Cutaneous barrier disruption followed by spore contamination and tissue invasion is a recognized route of infection for *Bacillus* spp. in humans (Pearson 1970), including a reported case of osteomyelitis (Schricker et al. 1994). Regarding *B. pumilus*, musculoskeletal infection has been described in human medicine, most notably as septic arthritis in a child in whom a minor penetrating injury was presumed to have introduced the bacterium into the joint, resulting in knee swelling, decreased range of motion, and pain (Shivamurthy et al. 2016). Although the iguana's plantar wound was in an advanced stage of healing, cutaneous *B. pumilus* infections have also been reported in individuals with no visible skin lesions (Tena et al. 2007), indicating that even subtle or unapparent disruptions of the integumentary barrier may enable bacterial entry. This is consistent with the proposed production of dermonecrotic factors by the bacterium, contributing to tissue invasion (Tena et al. 2007); however, the pathogenic mechanisms of *B. pumilus* remain poorly understood. When considering alternative routes of infection, acute food poisoning has been attributed to toxin-producing *B. pumilus* in humans (From et al. 2007, Shah et al. 2019). This route appears unlikely in the present iguana, as reported cases are typically characterized by gastrointestinal signs.

CONCLUSION

Acute unilateral knee swelling in green iguanas should prompt consideration of osteomyelitis as a differential diagnosis. Lizards affected by osteomyelitis should be closely monitored using imaging modalities, as radiographic and ultrasonographic changes may be more dramatic than clinical signs. In the present case, the decision to proceed with amputation was not delayed due to the rapid progression of osteolysis and osteoproliferation, which was likely pivotal in achieving local control of the infection. In addition, *Bacillus pumilus* should be considered a potential pathogen in infections in green iguanas, and possibly other lizard species, especially when repeatedly isolated from the lesion focus and sampled during open biopsy. In this sense, the present case report highlights the potential role of opportunistic environmental bacteria in musculoskeletal infections of captive lizards.

Acknowledgments.- This case report was funded by grant no. 2023/01363-1, "Fundação de Amparo à Pesquisa do Estado de São Paulo" (FAPESP).

Conflict of interest statement.- The authors declare no conflict of interest.

Credit author statement.- Conceptualization and Methodology: AAJ, FG, MARF, ABC; Writing – original draft: AAJ, ACME; Visualization: AAJ, ACME, FG, RFS, MARF; Investigation: AAJ, PGMR, FG, RFS, MARF, ACB; Writing – Review and Editing: AAJ, ACME, PGMR, FG, RFS, MARF, ABC; Supervision: MARF, ABC.

Data availability statement.- The data used in this case report are available and can be accessed upon request to the corresponding author at carregro@usp.br.

Editor-in-Chief.- Fabiano José Ferreira de Sant'Ana.

REFERENCES

Ballas P, Gabler C, Wagener K, Drillich M, Ehling-Schulz M. Characterization of *Bacillus pumilus* strains isolated from bovine uteri. Animals 2023; https://doi.org/10.3390/ani13081297

Banerjee C, Bustamante CI, Wharton R, Talley E, Wade JC. Bacillus infections in patients with cancer. Arch Intern Med 1988; https://doi.org/10.1001/archinte.1988.00380080059017

Bisetto SP, Justo AA, Bressan TF, Leal WP, Carregaro AB. Daily and seasonal features in the hind limb withdrawal latency of tegus (*Salvator merianae*) and green iguanas (*Iguana iguana*). J Therm Biol 2025; https://doi.org/10.1016/j.jtherbio.2025.104099

Borsa BA, Aldag ME, Tunali B, Dinç U, Dalar ZG, Özalp VC. A sepsis case caused by a rare opportunistic pathogen: *Bacillus pumilus*. Mikrobiyol Bul 2016; https://doi.org/10.5578/mb.27575

Celandroni F, Salvetti S, Gueye SA, Mazzantini D, Lupetti A, Senesi S, Ghelardi E. Identification and pathogenic potential of clinical bacillus and paenibacillus isolates. PLoS One 2016; https://doi.org/10.1371/journal.pone.0152831

Chinadurai SK, DeVoe RS. Selected infectious diseases of reptiles. Vet Clin North Am Exot Anim Pract 2009; https://doi.org/10.1016/j.cvex.2009.06.008

Clark AE, Kaleta EJ, Arora A, Wolk DM. Matrix-assisted laser desorption ionization–time of flight mass spectrometry: a fundamental shift in the routine practice of clinical microbiology. Clin Microbiol Rev 2013; https://doi.org/10.1128/cmr.00072-12

Davis AK, Maney DL, Maerz JC. The use of leukocyte profiles to measure stress in vertebrates: a review for ecologists. Funct Ecol 2008; https://doi.org/10.1111/j.1365-2435.2008.01467.x

Divers SJ, Redmayne G, Aves EK. Haematological and biochemical values of 10 green iguanas (*Iguana iguana*). Vet Rec 1996; https://doi.org/10.1136/vr.138.9.203

Ehinger AM, Meyer-Lindenberg A, Vick M, Nolte I, Kietzmann M. Concentration of enrofloxacin and its metabolite ciprofloxacin in canine matrices of the locomotor system. J Vet Med 2002; https://doi.org/10.1046/j.1439-0442.2002.jv411.x

Ferreira TH, Mans C. Evaluation of neuraxial anesthesia in bearded dragons (*Pogona vitticeps*). Vet Anaesth Analg 2019; https://doi.org/10.1016/j.vaa.2018.09.001

Filogonio R, Rodrigues GJ, Leite CAC. Ontogenetic scaling of the baroreflex function in the green iguana (I*guana iguana*). Am J Physiol Regul Integr Comp Physiol 2022; https://doi.org/10.1152/ajpregu.00037.2022

From C, Hormazabal V, Granum PE. Food poisoning associated with pumilacidin-producing *Bacillus pumilus* in rice. Int J Food Microbiol 2007; https://doi.org/10.1016/j.ijfoodmicro.2006.11.005

Ghussn LR, Justo AA, Sanches MC, Cortopassi SRG, Carregaro AB. Comparison between a tail clamp and electrical stimulation for sevoflurane minimum anesthetic concentration determination in green iguanas (*Iguana iguana*). J Am Assoc Lab Anim Sci 2024; https://doi.org/10.30802/AALAS-JAALAS-23-000124

Girling SJ, Fraser MA. Systemic mycobacteriosis in an inland bearded dragon (*Pogona vitticeps*). Vet Rec 2007; https://doi.org/10.1136/vr.160.15.526

Gise BT, Thorbrogger CJ, Rasys AM, Quandt JE, Divers SJ. Lizard anesthesia—a retrospective study of anesthetic protocol and monitoring quality of anesthetic episodes at a veterinary hospital over 23 years (2000–2023). Am J Vet Res 2025; https://doi.org/10.2460/javma.24.11.0728

Guagnoni IN, Armelin VA, Braga VHS, Monteiro DA, Florindo LH. Cardiovascular responses and the role of the neurohumoral cardiac regulation during digestion in the herbivorous lizard Iguana iguana. J Exp Biol 2024; https://doi.org/10.1242/jeb.247105

Heatley JJ, Russell KE. Hematology, p.301-318. In: Divers SJ, Stahl SJ. Mader's Reptile and Amphibian Medicine and Surgery. 2019; https://doi.org/10.1016/B978-0-323-48253-0.00033-7

Holmes SP, Divers SJ. Radiography—Lizards, p.491-502. In: Divers SJ, Stahl SJ. Mader's Reptile and Amphibian Medicine and Surgery. 2019; https://doi.org/10.1016/B978-0-323-48253-0.00054-4

Isaza R, Garner M, Jacobson E. Proliferative osteoarthritis and osteoarthrosis in 15 snakes. J Zoo Wildl Med 2000; https://doi.org/10.1638/1042-7260(2000)031[0020:POAOIS]2.0.CO;2

Justo AA, Sanches MC, Sladky KK, Lima CFM, Carregaro AB. Psychometric properties of a behavioral sedation scale for green iguanas (*Iguana iguana*). J Am Assoc Lab Anim Sci 2026; https://doi.org/10.30802/AALAS-JAALAS-26-060

Kimouli M, Vrioni G, Papadopoulou M, Koumaki V, Petropoulou D, Gounaris A, Friedrich AW, Tsakris A. Two cases of severe sepsis caused by *Bacillus pumilus* in neonatal infants. J Med Microbiol 2012; https://doi.org/10.1099/jmm.0.033175-0

Knafo SE. Musculoskeletal system, p.894-916. In: Divers SJ, Stahl SJ. Mader's Reptile and Amphibian Medicine and Surgery. 2019; https://doi.org/10.1016/B978-0-323-48253-0.00081-7

Kramer MH. Granulomatous osteomyelitis associated with atypical mycobacteriosis in a bearded dragon (*Pogona vitticeps*). Vet Clin North Am Exot Anim Pract 2006; https://doi.org/10.1016/j.cvex.2006.05.007

Neves-Maia J, Ramos MJ, Cruz H, Meireles M. *Bacillus pumilus* cellulitis with bacteremia in a person who injects drugs, living with HIV–HCV co-infection: a case report. Access Microbiol 2024; https://doi.org/10.1099/acmi.0.000398

Pearson HE. Human infections caused by organisms of the Bacillus species. Am J Clin Pathol 1970; https://doi.org/10.1093/ajcp/53.4.506

Robinson JE, Griffiths RA, John FAV, Roberts DL. Dynamics of the global trade in live reptiles: Shifting trends in production and consequences for sustainability. Biol Conserv 2015; https://doi.org/10.1016/j.biocon.2014.12.019

Schricker ME, Thompson GH, Schreiber JR. Osteomyelitis due to *Bacillus cereus* in an adolescent: case report and review. Clin Infect Dis 1994. https://doi.org/10.1093/clinids/18.6.863

Shah MM, Miringu G, Wada A, Kaneko S, Ichinose Y. Case report: *Bacillus pumilus*–caused bacteremia in a patient with food poisoning. Am J Trop Med 2019; https://doi.org/10.4269/ajtmh.18-0593

Shivamurthy VM, Gantt S, Reilly C, Tilley P, Guzman J, Tucker L. *Bacillus pumilus* septic arthritis in a healthy child. Can J Infect Dis Med Microbiol 2016; https://doi.org/10.1155/2016/3265037

Stahl SJ. Pet lizard conditions and syndromes. Semin Avian Exot Pet Med 2003; https://doi.org/10.1053/saep.2003.00019-7

Tena D, Matínez-Torres JÁ, Pérez-Pomata MT, Sáez-Nieto JA, Rubio V, Bisquert J. Cutaneous infection due to *Bacillus pumilus*: report of 3 cases. Clin Infect Dis 2007; https://doi.org/10.1086/511077

Thabit AK, Fatani DF, Bamakhrama MS, Barnawi OA, Basudan LO, Alhejaili SF. Antibiotic penetration into bone and joints: an updated review. Int J Infect Dis 2019; https://doi.org/10.1016/j.ijid.2019.02.005

Vaillard J, Aguilar LAB, Bernal AM, Racine IM, Cícero RWC, Ramos Garduño LA. Septic arthritis and granulomatous osteomyelitis in a bearded dragon (*Pogona vitticeps*) caused by *Mycobacterium* sp. J Herpetol Med Surg 2021; https://doi.org/10.5818/JHMS-S-20-00009

Vetere A, Bertocchi M, Pelizzone I, Moggia E, Gerosa S, Di Ianni F. *Klebsiella* sp.-related infectious spondylitis in a bearded dragon (*Pogona vitticeps*). BMC Vet Res 2021; https://doi.org/10.1186/s12917-021-02933-7

Figures

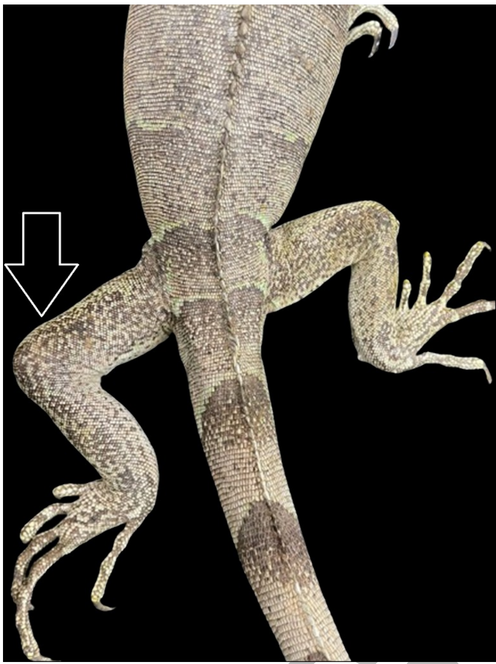

Fig. 1. Dorsoventral view of the pelvic limbs of a green iguana showing diffuse swelling of the left hindlimb, particularly at the knee (arrow), compared with the contralateral limb.

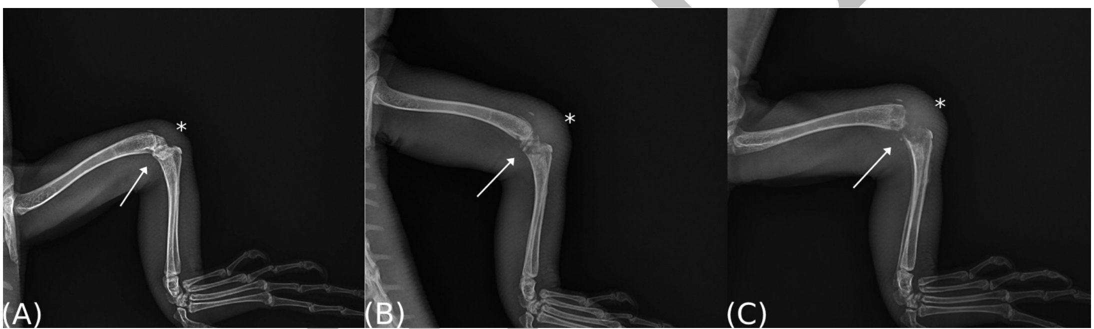

Fig. 2-4. Lateromedial radiographic view of the left pelvic limb. (**2**) Day 1 of treatment. Mildly increased soft tissue volume (asterisk) in the left femorotibiopatellar joint (arrow). (**3**) Ten days after the initial examination. Marked increase in soft tissue volume of the femorotibiopatellar joint (asterisk) compared with the previous examination, cortical thinning of the distal femoral epiphysis, and radiolucent lytic areas in the proximal tibial epiphysis (arrow). (**4**) Thirty days after the initial examination. Poorly defined margins and extensive bone lysis involving the distal femoral and proximal tibial epiphyses (arrow), with persistent soft tissue swelling of the femorotibiopatellar joint (asterisk).

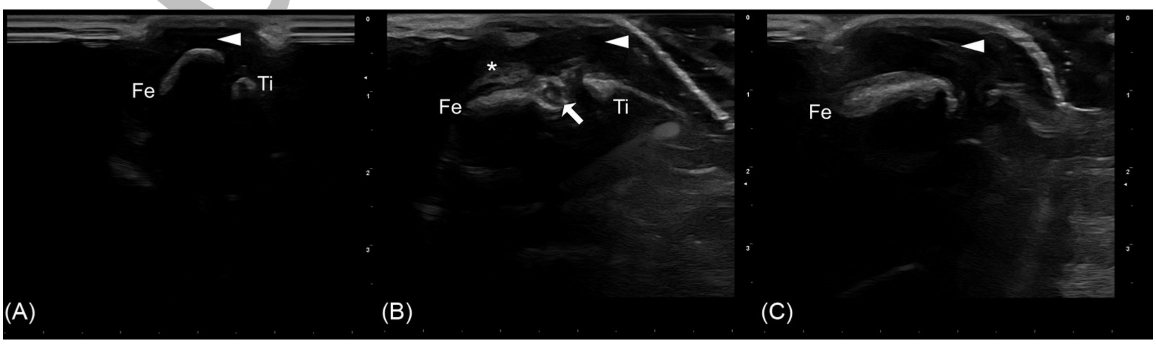

Fig. 5-7. Longitudinal ultrasonographic images of the left femorotibiopatellar joint demonstrating progression of osteoarticular disease and joint effusion. Anechoic fluid within the joint is indicated by white arrowheads. (**5**) Day 1 of treatment. Regular hyperechoic lines with distal acoustic shadowing corresponding to the cortical

surfaces of the femur (Fe) and tibia (Ti). (**6**) Ten days after the initial examination. Irregular hyperechoic cortical surfaces with osteolytic (arrow) and osteoproliferative (asterisk) changes adjacent to the femur (Fe) and tibia (Ti). (**7**) Thirty days after the initial examination. Marked distortion of the hyperechoic cortical surface of the distal femoral epiphysis (Fe) and loss of definition of the proximal tibial surface, accompanied by marked accumulation of anechoic fluid within the joint.

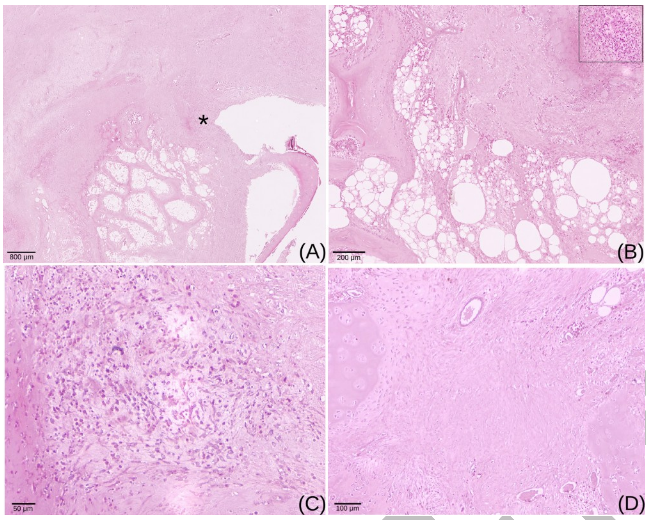

Fig. 8-11. Histopathology of the affected femorotibiopatellar joint and adjacent bone. (**8**) Low-magnification view demonstrating moderate periosteal lysis and proliferation (asterisk). HE, obj. 2x. (**9**) Extensive fibroplasia (square) replacing portions of the trabecular bone, articular cartilage, and joint capsule. HE, obj. 4x. (**10**) Higher-magnification view of the fibroplasia shown in Figure 9. HE, obj. 20x. (**11**) Fibrous connective tissue extending into adjacent bone and cartilage. HE, obj. 10x.

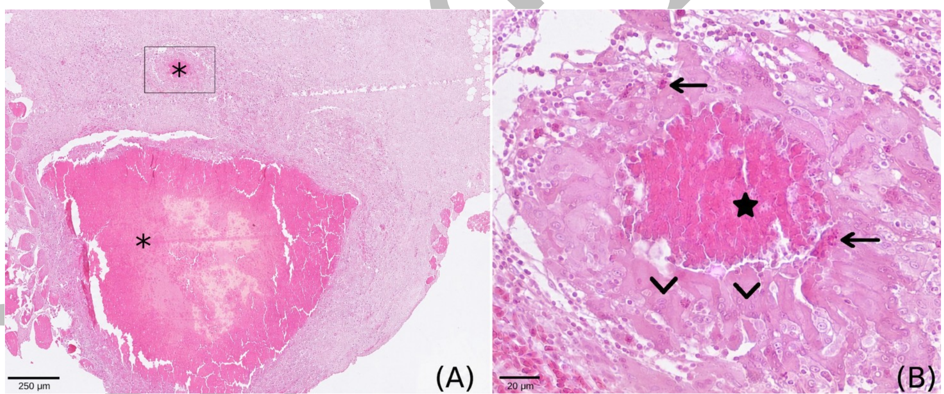

Fig. 12-13. (**12**) Multiple granulomas were found in the surrounding subcutaneous tissue and muscle (asterisks). The rectangle represents the area shown in Figure 13. HE, obj. 4x. (**13**) Granulomas were composed of a central area of necrosis (solid star) with necrotic debris and granulocytes (solid arrows) surrounded by mononuclear and multinucleated giant cells (arrowheads). HE, obj. 40x.

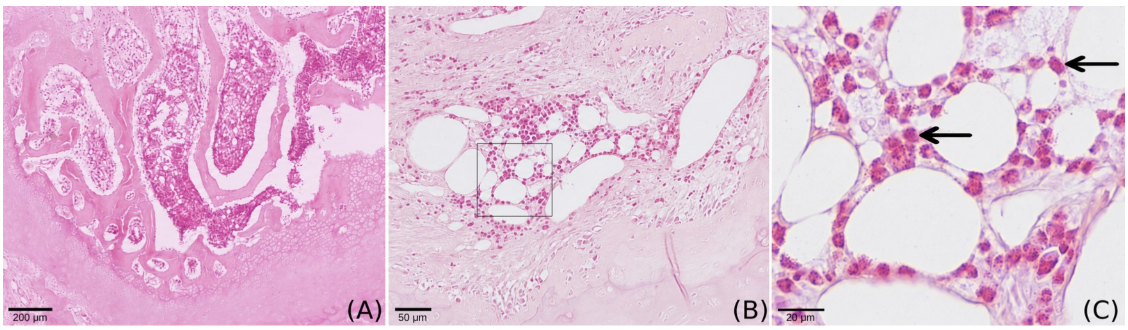

Fig. 14-16. Histopathology demonstrating (**14**) extensive granulocytic infiltration replacing bone marrow (HE, obj. 4x), (**15**) and infiltrating adjacent fibrous tissue (HE, obj. 10x). (**16**) Higher-magnification view of the square in Figure 15, highlighting the dense granulocytic infiltrate (arrows). HE, obj. 40x.

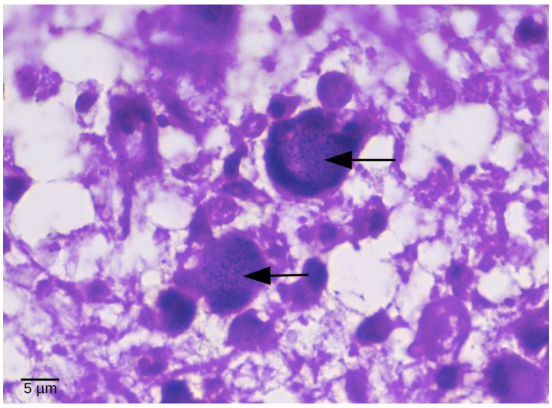

Fig. 17. Gram-positive structures morphologically consistent with bacteria within the cytoplasm of multinucleated giant cells (solid arrow). HE, obj. 100x.